LAWRENCE
LIVERMORE
NATIONAL
LABORATORY

LLNL-TR-416167

Thermal Modeling and Feedback Requirements for LIFE Neutronic Simulations

J. E. Seifried

August 26, 2009

Disclaimer

This work performed under the auspices of the U.S. Department of Energy by Lawrence Livermore National Laboratory under Contract DE-AC52-07NA27344.

Thermal Modeling and Feedback Requirements for LIFE Neutronic Simulations

Jeffrey Seifried
Lawrence Livermore National Laboratory
jeffseif@berkeley.edu

August 7, 2009

Abstract

An initial study is performed to determine how temperature considerations affect LIFE neutronic simulations. Among other figures of merit, the isotopic mass accumulation, thermal power, tritium breeding, and criticality are analyzed. Possible fidelities of thermal modeling and degrees of coupling are explored. Lessons learned from switching and modifying nuclear datasets is communicated.

1 Introduction

1.1 Main Questions

In the summer of 2008, the Laser ICF Fission Energy (LIFE) neutronics group was concerned about the necessity of thermal modeling and feedback for LIFE neutronic simulations. At that point in time, most life-cycle runs of LIFE designs were performed at time-invariant and spatially-uniform temperatures; only nuclear data produced for a single temperature was used for transport and depletion. There were concerns about whether this could impact the success of a simulated design. These concerns are identified more explicitly below.

1. Can thermal modeling and feedback (or the lack thereof) affect the results of a simulated design?
2. How sensitive are the results of a LIFE simulation to temperature considerations?
3. What is the necessary fidelity of thermal modeling and degree of coupling?

The first question is addressed with a coarse scoping study and analysis of the resultant figures of merit that were identified with respect to the ability of a LIFE design to achieve its core missions. The second question can be addressed when finer, more physically realistic calculations are performed (for feedback coefficients, acceptable error tolerances for temperatures, etc.). The third question could be answered for current and future LIFE designs after the sensitivities are known and physical processes are understood.

1.2 Motivation

The typical light-water reactor is a critical thermal nuclear reactor. During operation, it balances various neutron sources and sinks to sustain a chain reaction that produces a constant thermal power. This can only be achieved when negative feedbacks from state variables stabilize operating conditions at their nominal values. Perturbations from the nominal values of fuel temperature, moderator temperature, and moderator density interact; operating conditions move in damped oscillations to steady-state conditions through inherent coupling mechanisms. This coupled nature of operation necessitates basic modeling of thermal-hydraulics to predict steady-state operating conditions. Generally, coarse models of all the coupled physics are sufficient to predict the integral behaviors of a light-water reactor (reactivity feedback is based on integral quantities such as core power, bulk coolant void coefficient, and bulk temperatures).

In Boiling Water Reactors, moderator voiding and isotopic enrichments can change significantly over small length scales to impact neutron flux, flow fields, and temperatures along the same length scales. In order to capture local phenomena such as power peaking, crud deposition, and intra-pin depletion, sophisticated high fidelity models are required. There are groups pursuing coupling neutron transport calculations with CFD for these purposes [1].

While a LIFE engine is quite different from a light-water reactor, basic coarse modeling is a good place to start when one considering the level of modeling and coupling that is necessary to accurately predict integral results for a coupled LIFE simulation.

2 Theory

2.1 Temperature's Effect on Resonance Reaction Rates

Temperature affects neutron transport primarily through Doppler broadening of resonances (and also low-energy scattering). Heavy nuclei contain numerous quantum resonant energy levels. Compound nuclei are more easily formed at one of these excited energy levels than another. Consequently, the probability of interaction of a neutron and a target nucleus is much larger when the relative kinetic energy of the particles is such that the compound nucleus will reside at a resonant energy after interaction. A plot of this probability of interaction versus neutron kinetic energy yields a dramatic increase in the sharp vicinity of this energy level, or a "resonance".

For a perfectly stationary target nucleus only neutrons of an exact energy level can create this resonant compound nucleus. The resonance is therefore of infinitesimal width, finite area, and infinite height. For a target nucleus of nonzero temperature, thermal vibrations smear or "broaden" the neutron kinetic energies that will resonate the compound nucleus. Since the compound nucleus' affinity for the quantum excitation energy is unchanged by thermal vibrations, the probability of interaction does not change and the area of the resonance remains constant and the height of the resonance is lowered. In Figure 1, the total neutron cross-section for uranium 238 is shown around its resonance of 6.67 eV. Point-wise data is extracted from nuclear data provided by Tom Marcille at LANL during summer 2008 at 300, 600, 900, 1200, and 1500 degrees Kelvin. The broadening and shortening of the resonance with temperature increase is evident.

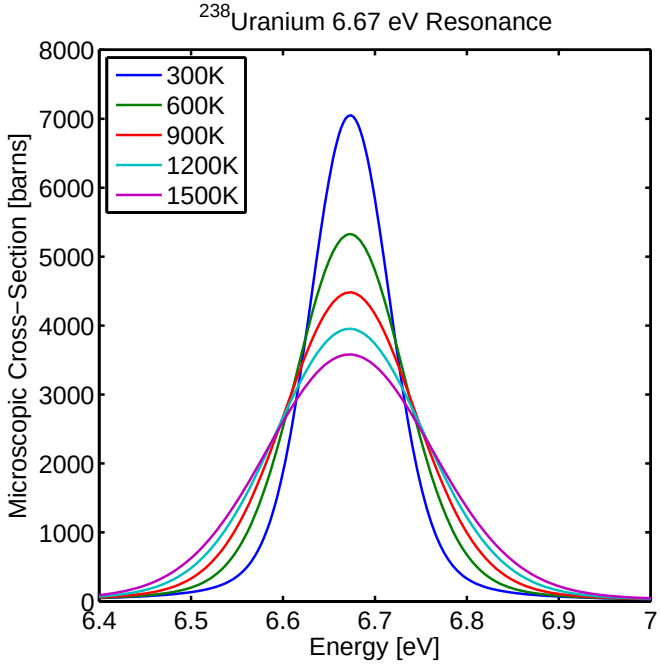

Figure 1: Doppler broadening of the uranium 238 6.67 eV resonance.

If a resonance is absorptive, neutrons at that energy are removed and the neutron flux is depressed in that energy region. The flux depressions at the boundaries of the resonance reduce further absorption towards the interior of the resonance. In effect, the resonance is shielding its self from its full reaction capacity. When temperature increases broaden and shorten resonances, this energy "self-shielding" is relieved. The result is a non-linear reduction in the self-shielding and a local increase of reaction rate with temperature [2, pp. 435–437]. In Figure 2 are actual results that show the qualitative behaviors of the neutron flux and reaction rate in the vicinity of a resonance due to thermal Doppler broadening at a low-energy resonance.

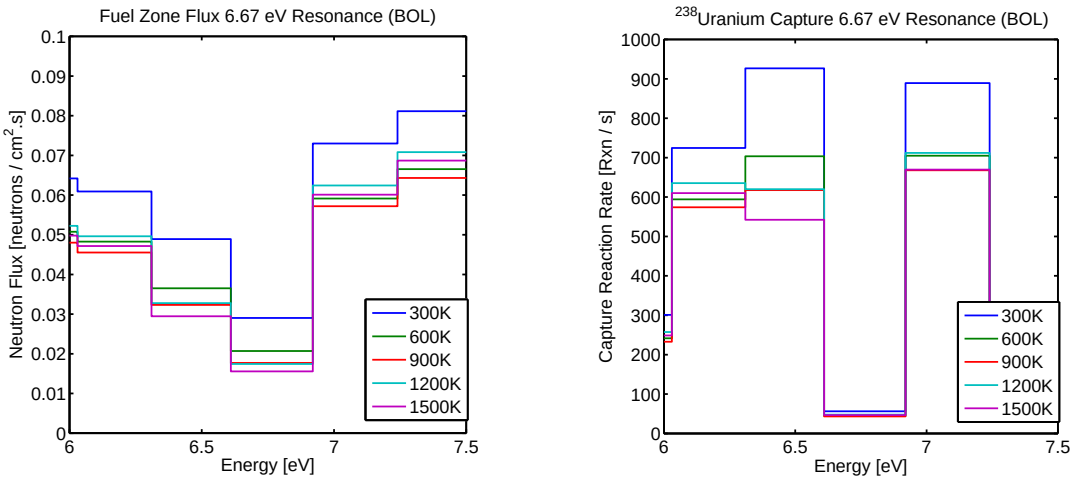

Figure 2: Energy self-shielding of (left) the neutron flux and (right) reaction versus temperature.

Red Cullen performed an initial analysis of temperature's effect on neutron transport, important reaction rates, and energy depositions [3]. His conclusion was that 3-4% differences in magnitude could eccur at different temperatures. These were not uncertainties, but biases in results. How these biases accumulate with depletion was not addressed explicitly, but it was speculated that they could result in moderate to drastic discrepancies at the middle and end of a life-cycle.

2.2 Degree of Thermal Coupling and Fidelity of Thermal Modeling

There are various degrees to which thermal calculations could be coupled to the transport and depletion calculations. They are summarized Table 1 in increasing expense and then expanded upon afterward. It should be noted that "TS" denotes the number of depletion outer burn steps in a life-cycle run.

# of Calculations Per Run	Scenario
<1	Generic temperature profile is used for every run
1	Temperatures are calculated once, prior to every run
TS $\div$ 5	Temperatures are updated every few time-steps
TS	Temperatures are updated every single time-step
TS $\times$ 10	Temperatures and transport are iterated until convergence every time-step

Table 1: Degrees of thermal coupling.

If physical coupling is weak, one can conceivably perform a single thermal calculation, from which a generic temperature profile could be obtained and applied to a class of LIFE designs. It would not make sense to have this calculation be of great fidelity unless the coupling is so weak that the details of the thermal results are prominent and unchanged throughout the class of problems. The fidelity of the thermal calculation can be adjusted by considering different levels of the physics, by using different sizes and explicitnesses of geometry, and by refining the fidelity and precision of the coupled neutronics calculation. The ideal fidelity would be the lowest fidelity that contributes error that is smaller or on the order of the errors and uncertainties from other aspects of the simulation. For example, the nuclear data and stochastic transport calculation contribute uncertainties and homogenization and depletion contribute errors.

With slightly stronger coupling, it might be appropriate to perform a single thermal calculation for each life-cycle run at the beginning of a run. Going another step, the calculation could be performed every few time steps or even every time step as a thermal update. As the coupling becomes stronger, the finer details of the physics become more important and merit more refined models. Depending on the nature of the system, a less frequent thermal update at a high fidelity might give similar results as a more frequent thermal update at a lower fidelity. In the extreme of tight coupling, the transport and temperature calculations could be iterated upon until convergence for every time step.

The degrees of coupling can also be combined in a hybrid manner. Different couplings could be applied for the modes of a life-cycle simulation if each possesses varying degrees of physical coupling. In general though, the thermal calculations can be performed with much less expense than transport and depletion calculations. Therefore, erring on the side of performing more thermal calculations at a higher fidelity than necessary is generally acceptable.

2.3 LIFE Thermal Simulation

Until now, thermal calculations were separated from the transport and depletion calculations (offline for maximum temperatures and stresses). Since they are manually intensive, they were performed only periodically and no element of feedback was used, with regard to thermal broadening of the nuclear data.

Currently, thermal calculations can be embedded into a life-cycle run. The process is automated through scripts that parse transport input and output and a T/H-specific input file, then perform some simple calculations. Resultant temperature and flow information is outputted to file for posterity, but online feedback via altering of nuclear data libraries has yet to be implemented. Figure 3 identifies the state of feedback implementation.

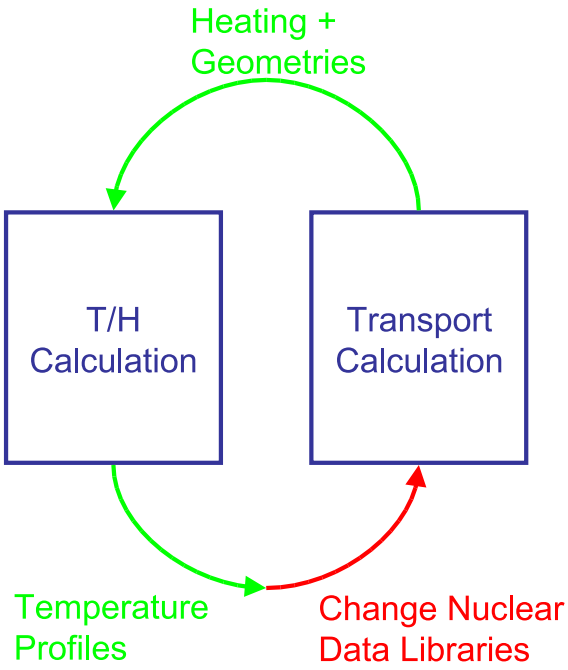

Figure 3: LIFE simulation thermal feedback including (blue) prior, (green) current, and (red) future implementations.

3 Methodology

3.1 Current T/H Calculation

The current thermal-hydraulic simulation is based upon a MathCad worksheet created by Ryan Abbott [4]. It employs a quasi-static, one-dimensional radial bulk heat transfer model. Essentially, the coolant is thermodynamically heated as it flows outward through the porous medium bed. Solid surface temperatures are calculated relative to the bulk coolant temperature through convective heat transfer; solid center-line temperatures are calculated relative to surface temperatures through conduction. The correlations are conditional upon geometry and flow type (plenum, porous plate, pebble, etc.).

In the MathCad worksheet materials, geometries, coolant inlet and outlet temperatures, and heatings were generated and specified manually. In the current model, all of that information is parsed from input and output files from the transport calculations. To get a feel for the fidelity of the calculation, the heating for a typical design and its resultant temperature profiles are shown in Figure 4. It should be noted that within each radial shell, the volumetric heating is assumed uniform. This simplification does not characterize the large volumetric heating gradients that occur in

the reactor and will be addressed in the future either through a higher fidelity transport calculation, or an assumed normalized distribution.

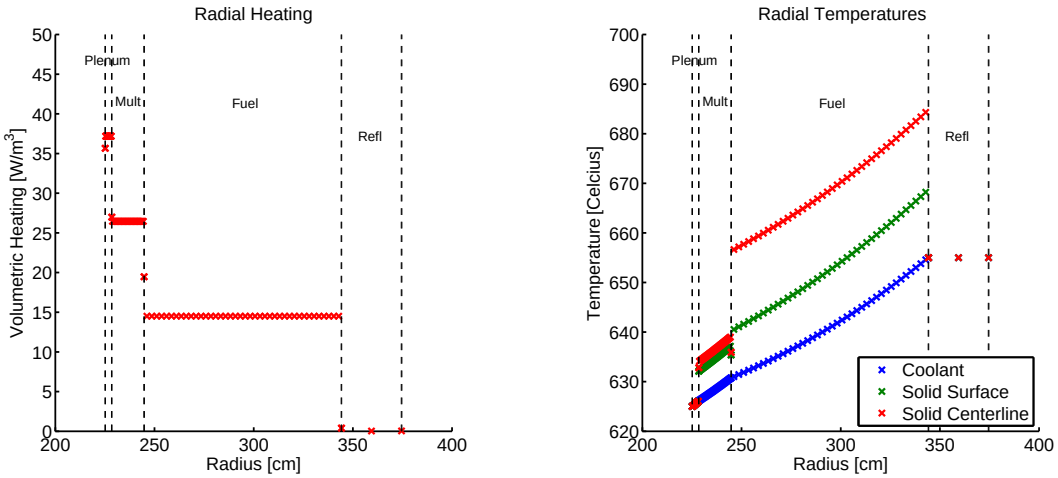

Figure 4: Example (left) thermal heating information and (right) resultant temperature profile.

3.2 Validation of T/H Calculation

A Fortran subroutine was written to perform an I/O step within the LNC. After each depletion step, the MCNP output file and other run-specific input files are parsed for necessary state variables including neutron and photon energy deposition tallies, cell masses, and fusion power. The neutron energy deposition and system thermal power are calculated and written to the file "power.out." The steps in this procedure overlap substantially with those necessary for performing an automated thermal calculation. It therefore was a candidate for an informal validation. Its functionality was incorporated into the thermal-hydraulic calculation script, with some convenient improvements. Refer to the memo for more information [5].

3.3 Nuclear Data Generation

Nuclear data distributed in ENDF format is freely available online [6, 7]. The most recent version includes 393 isotopes, for a total of 1.7 GB of data. The ENDF format contains resonance parameters and high-order interpolation schemes for compactness and generality. MCNP requires data to be point-wise, such as in an ACE format. NJOY is a software package that serves to convert nuclear data from ENDF to ACE format.

It should be noted that the conversion process is complicated and not standardized. There are several steps that can be performed at arbitrary precision, with various physics turned on or off [3, 8]. Some example steps are linearization of data, construction and broadening of resonances, generation of reactions, linearization of Legendre tables, and checking consistency of cross-sections. Much of the art of nuclear data analysis lay within these steps.

3.4 Validation of Marcille's Nuclear Data

In the summer of 2008, 47GB of ACE-formatted data was provided by Tom Marcille at LANL. It was broadened to 30 temperatures between 300K and 2800K (in contrast to the former data that contained only one temperature). Before the data could be used with confidence, it had to be compared with existing qualified data that was assumed accurate.

Data generated by Tom Marcille, Peter Song and Red Cullen were used in a homogenized TRISO criticality problem in MCNP. In addition, Red Cullen's data was used in an analogous criticality problem in TART. The k_{eff} and various reaction rates were chosen as the figure of merit. Nuclear data sets were also compared qualitatively by plotting of the point-wise cross-sections. Refer to the memo for more information [9].

3.5 Significance of Temperature Effects on a Life-Cycle

The significance of temperature effects on a life-cycle was addressed with bounding scoping studies. Full life-cycle runs were performed on a depleted uranium case with nuclear data provided by Marcille at 300K, 600K, 900K, 1200K,

and 1500K. The important figures of merit of thermal power, tritium breeding ratio (TBR), tritium mass, actinide mass, and burnup. Additionally, the masses of important isotopes were extracted. The "important" isotopes were selected on a basis of relevance to important reaction rates (fission, tritium production, parasitic capture, etc.), and waste repositories. The selected isotopes are tabulated in Table 2.

Isotope	ZA ID
^{6}Li ^{7}Li	3006 3007
^{93}Zr	40093
^{99}Tc	43099
^{106}Pd	46106
^{126}Sn	50126
^{127}I ^{129}I ^{131}I ^{135}I	53127 53129 53131 53135
^{128}Xe ^{129}Xe ... ^{135}Xe ^{136}Xe	54128 54129 ... 54135 54136
^{135}Cs ^{137}Cs	55135 55137
^{147}Sm ^{148}Sm ... ^{153}Sm ^{154}Sm	62147 62148 ... 62153 62154
^{235}U ^{236}U ^{237}U ^{238}U ^{239}U	92235 92236 92237 92238 92239
^{237}Np ^{238}Np ^{239}Np	93237 93238 93239
^{236}Pu ^{237}Pu ... ^{242}Pu ^{243}Pu	94236 94237 ... 94242 94243
^{241}Am ^{242}Am ^{243}Am ^{244}Am	95241 95242 95243 95244
^{242}Cm ^{243}Cm ... ^{247}Cm ^{248}Cm	96242 96243 ... 96247 96248

Table 2: Important isotopes.

Energy-dependent neutron flux and important reaction rates (fission and radiative capture) were tallied for a subset of the heavy "important" isotopes and tritium production and neutron multiplication was tallied for a subset the light "important" isotopes. Doppler feedback coefficients were calculated, using the original nuclear data (Song) for depletion and the Marcille data for k_{eff} . All of these calculations were performed at the beginning of life, the time step of peak Pu, and 99% burnup (when achieved).

4 Results

4.1 Validation of T/H Calculation

Results were virtually identical for all figures of merit, for all four cases. Optimized contextual parsing with regular expressions improved robustness and removed the required inputs to reduce human error potential. See the memo for more details [10].

4.2 Validation of Marcille's Nuclear Data

As discussed in the related memo [9], the k_{eff} 's compare very well between the two data sets, when within the context of the various transport codes, and when the correct temperatures are considered.

Nuclear data from Marcille and Song contain mostly the same isotopes. There are, however, a handful of differences that are summarized in Table 3. All missing data must be incorporated into the library and referenced by the xsdir or removed from any input files and mbxs.inp's.

Additionally, a few useful MT reactions are omitted from each library for specific isotopes (Table 4). If attempts are made to tally these missing MT #'s (or other missing MT #'s), a quiet warning is be sent to stdout (among the other dozens of warnings) and the tally will return 0. Since these cards are embedded within the ACE formatted data, they cannot be imported differently from the rest of the data, supplemented with other files. Although tedious, it may be possible to manually recreate these desired tallies, since they are the sum of several other tallies.

4.3 Significance of Temperature Effects on a Life-Cycle

4.3.1 Spectral results

The energy-dependent fluxes and reaction rate distributions are located in Appendix A.

Marcille XS	Song XS	Both XS
^{253}Es	^{231}Pa	^{12}C
.	^{233}Pa	^{13}C
.	^{249}Ca	^{20}Ne
.	.	^{231}Th
.	.	^{Nat}Si
.	.	photon
.	.	electron

Table 3: Cross-sections missing from data libraries.

Marcille 105	Marcille 205	Song 105
^{7}Li	^{6}Li	^{7}Li
.	^{7}Li	.
.	^{9}Be	.

Table 4: MT reactions missing from data libraries.

4.3.2 Criticality & Doppler feedback coefficients

Song's data was used for depletion. Temperature branching calculations were performed for k_{eff} with the Marcille data at several time steps, including the beginning of life (0), maximum plutonium mass (63), and 99% burnup (293). The results of these branching calculations are shown in Table 5 (uncertainties are shown in pcm).

Time step	300K	600K	900K	1200K	1500K	Song
0	0.03727 ± 1	0.03630 ± 1	0.03561 ± 1	0.03504 ± 1	0.03457 ± 1	0.03628 ± 1
63	0.54371 ± 13	0.53368 ± 13	0.52681 ± 12	0.52176 ± 12	0.51738 ± 12	0.53411 ± 13
120	0.52426 ± 12	0.51610 ± 12	0.51110 ± 12	0.50692 ± 17	0.50371 ± 12	0.51663 ± 12
180	0.48416 ± 12	0.47694 ± 12	0.47213 ± 12	0.46864 ± 12	0.46568 ± 11	0.47737 ± 12
240	0.30253 ± 11	0.29853 ± 11	0.29590 ± 11	0.29392 ± 10	0.29267 ± 11	0.29846 ± 11
291	0.05550 ± 2	0.05519 ± 2	0.05505 ± 2	0.05494 ± 2	0.05489 ± 2	0.05508 ± 2

Table 5: keff versus temperature for various time steps.

The Doppler feedback coefficients calculated with these k_{eff} 's using the formula

$$\alpha_T \equiv \frac{1}{\text{mean}\,(k^2)} \cdot \left(\frac{\partial k}{\partial T}\right)_{\text{least-squares}}$$

are shown in Table 6 versus time step along with the corresponding average k_{eff} (with uncertainty in pcm).

Time step	$\alpha_T \left[\frac{\text{pcm}}{\text{K}}\right]$	$<k_{eff}>\pm$[pcm]
0	-173.50	0.035758 ± 1
63	-7.6998	0.52867 ± 12
120	-6.3817	0.51242 ± 13
180	-6.7275	0.47351 ± 12
240	-9.2108	0.29671 ± 11
291	-16.131	0.055114 ± 2

Table 6: Doppler coefficients and average keff for various time steps.

4.3.3 Isotopic results

The isotopic histories for the "important" isotopes can be found in Appendix B in graphical form.

4.3.4 Integral results

The integral results for thermal power, TBR, accumulated tritium mass, total actinide mass, and burnup (FIMA) can be found in Appendix C. Results from the five temperature runs and those of Song's data are included.

5 Discussion

5.1 Validation of T/H Calculation

Although the exercise presented only a partial validation of the T/H calculation, the identical results build confidence that the calculations perform their functions in an identical, predictable way [10].

5.2 Validation of Marcille's Nuclear Data

5.2.1 MCNP Calculation

While the validation addressed the ratio (not the magnitudes) of some important reaction rates for a related problem (k_{eff}), many aspects of the data libraries were not compared. For example neither the energy deposition tallies nor tritium production reaction rates were compared even though both are critical to a LIFE simulation. Since the test problem was of homogenized geometry, scattering cross-sections (although significantly less important than energy deposition and tritium production) were not compared.

Essentially, the 'validation' was very high-level and several additional steps would be required to validate a nuclear data set versus another (or versus experiment). Ideally an automated tool could directly calculate differences and ratios of the cross-sections rather than the slow process of using them in transport calculations. Finally, whether or not the absence of portions of nuclear data libraries can affect the results of transport would need to be addressed.

5.2.2 Nuclear Data Issues

The Marcille data was initially used naively without verification and validation. Unfortunately the date contained many instances of meaningless negative numbers, most of which have since been scrubbed. The scrubbing process was not exhaustive (although it was tedious and had to be automated through extensive use of scripting). A program CHECKXS.exe was provided along with the nuclear data that, among other things, removed all occurrences of '-2147483684' (2^{-31}) which was introduced by NJOY during processing. Even though the data is no longer used, the reasons for the scrubbing process not being exhaustive are outlined for posterity.

There are 398 original data libraries and 397 are successfully parsed by the scrubbing program (Fe-56 freezes during runtime). Among the completed parsings, 139 of the outputs indicate the need to replace erroneous data, while only 138 scrubbed libraries are created (Bi-209 crashes during runtime). Among the libraries that were not deemed scrub-worthy, 68 still contain occurrences of '-2147483684' (not ^{166m}Ho or ^{115m}Cd). Among the scrubbed libraries, 67 still contain '-2147483684' (not ^{150}Nd, ^{160}Dy, or ^{290}Bi). Clearly this situation is confusing and not ideal as occasionally runs will fail upon colliding with a erroneous data point.

The libraries files were grouped by isotope, which meant that all 30 temperatures were placed within a single file. These enormous files (1.7GB for ^{232}Th) caused great slowdown in runtime, on the order of 3–10X. The relevant data blocks have since been extracted to smaller, individual files. The missing or incorrect tally multipliers suggest there may been even more undiscovered errors. Perhaps it makes more sense to generate a fresh data set, with a clear understanding (hopefully) and documentation of the assumptions made. The decision needs to be made before the data can be seriously considered as the primary set: will it undergo an exhaustive benchmark, or will it be abandoned for self-generated data?

5.3 Significance of Temperature Effects on a Life-Cycle

5.3.1 Spectral effects

The flux spectrum throughout the reactor is sensitive to temperature (Figure 9). In the vicinity of all major resonances, flux and reaction rate depressions are reduced as temperature increases (Figures 10, 11, 12, 13, and 14). This results in

globally increased resonance absorption that reduces flux in the slowing-down energies and starves thermal energies from neutrons. Additionally, the thermal neutron hump is shifted upwards with temperature. Consequently, reactions are shifted from thermal energies to resonance energies as temperature increases.

At first glance of the initial time-step results, the variation of thermal neutron spectrums with temperature makes absolutely no sense: the 300K flux was higher than the rest and 600K/900K and 1200K/1500K coincided. However, when one looks more closely, they find that the amount of ^{6}Li in the system is 20.5kg for 300K, 26.7kg for 1200K and 1500K, and 75.9kg 600K and 900K. These quantities do not reflect any trend with temperature. Rather, they are artifacts of the deterministic tritium control iteration scheme at the initial time-step: 300K took 6 iterations, 600K and 900K took 10, and 1200K and 1500K took 5. Since ^{6}Li has such an enormous thermal cross-section (Figure 5), its presence has a large affect on the thermal flux (and therefore reaction rates) and outweighs the aforementioned inherent physical effects.

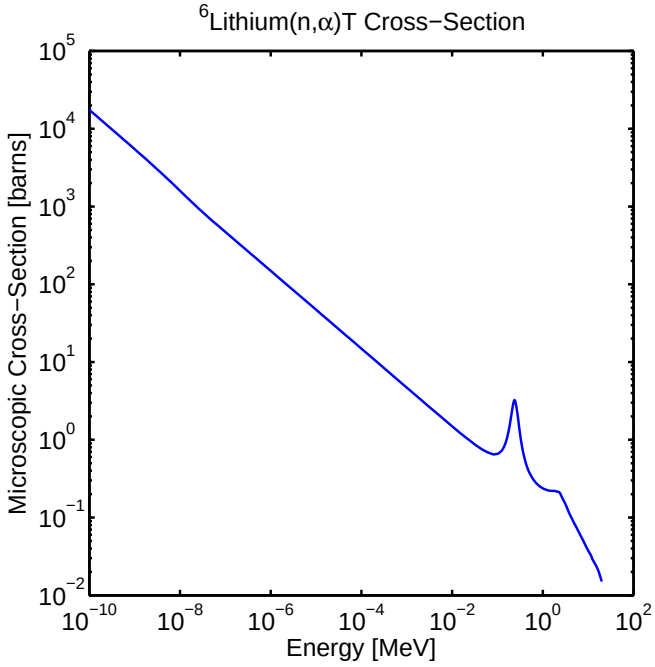

Figure 5: Lithium-6 tritium production cross-section.

At the time of peak plutonium, the lithium concentration perturbations are small and the inherent thermal flux reduction and hump shift are more visible. Even though differing isotopic inventories complicate reaction rate results, some clear trends can be identified. All tabulated heavy-metal reaction rates were diminished at thermal energies; thermal flux variations outweighed isotopic variations. All reaction rates at high energies were approximately constant with temperature except for ^{235}U, whose mass increased $\sim$30% for 300K$\rightarrow$1500K.

At 99% burnup, all of the fluxes converged and reaction rates were universally lower for the higher temperature runs, which had smaller remaining inventories of the tabulated materials. If the tabulated inventories were expanded to include higher actinides, one would find increased abundances of those isotopes and therefore reaction rates at higher temperatures.

^{9}Be$(n,2n)$ reaction rates (a threshold reaction) were virtually unchanged by temperature (Figure 15) throughout the life-cycle.

5.3.2 Criticality & Doppler feedback coefficients

The depleted uranium-fueled LIFE engine remained deeply sub-critical for the duration of the life-cycle (beginning at $\sim\frac{1}{18}$ and peaking at $\sim$0.55). The differences in k_{eff} between Marcille 600K data and Song data were never within the uncertainty, but were always close; differences were in the 10's of pcms, while uncertainties were $\sim$10 pcm. Differences between the k_{eff} of adjacent temperatures were always larger than the uncertainty, often 40x or so. While the criticality of a single inventory is slightly sensitive to temperature changes (Doppler feedback coefficients were large and negative [2, pp. 562–563]), diverged inventories (from depleting at different temperatures) would have a

larger effect upon criticality (and less-so, the Doppler feedback coefficient) (Figure 6).

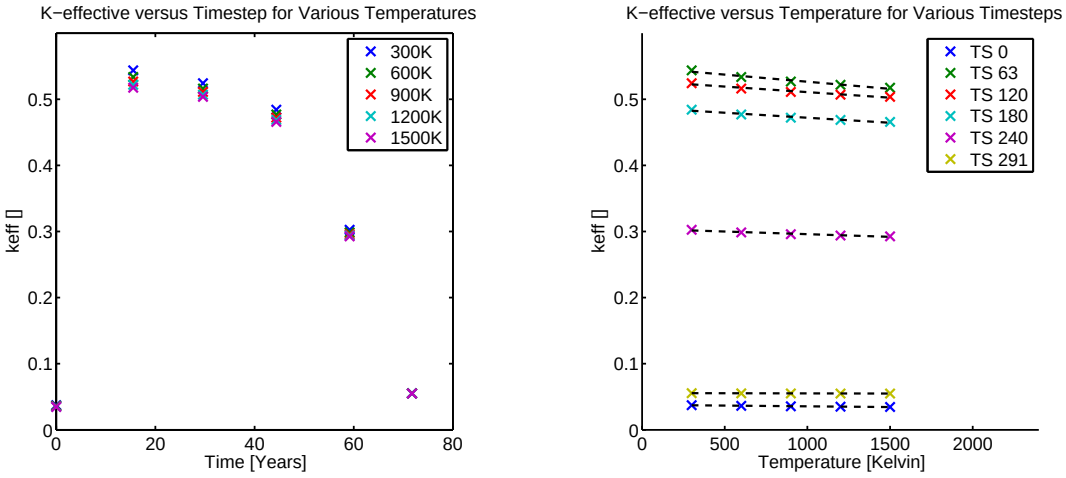

Figure 6: K-effective (left) versus for Various Temperatures and (right) versus Temperature for Various Time-Steps.

5.3.3 Isotopics

The 56 isotopes that were identified as 'important' can be put into a few general classes (or hybrids of them) based on extrema of mass time-history behaviors. If one writes a simplified conservation equation (decay loss, neutronic destruction loss, decay sources, fission + absorption sources) for an isotope X:

$$\frac{\partial X}{\partial t} = -X \cdot (\lambda_x + \phi \cdot \sigma_{a,x}) + (\text{decay sources}) + (\text{fission constants}) \cdot \gamma_x \cdot P_{thermal},$$

it becomes clear that three main parameters define these behaviors: the decay constant (λ_x), the destruction cross-section ($\sigma_{a,x}$), and the fission yield (γ_x). Additionally, the spectrum of neutron flux (ϕ) and the magnitude of thermal power ($P_{thermal}$) serve as forcing functions.

The class 'long-lived fission products' includes isotopes with a modest fission yield that are stable or extremely long-lived (compared to the ∼70 year life-cycle), and have low to modest destruction cross-sections (∼1–10 barns with no significant resonances). Since their major sources are from fission and they have extremely small decay and destruction losses, their time-derivative is essentially proportional to the thermal power. ^{93}Zr (Figure 16) serves as an excellent example of this class that also includes ^{106}Pd, ^{129}Xe, ^{130}Xe, ^{132}Xe, ^{134}Xe, ^{136}Xe, ^{137}Cs, and ^{148}Sm.

The class 'hump isotopes' includes isotopes that are produced by fission or bred, possessing a medium half-life (∼years) or a modest destruction cross-section (∼500–10,000 barns). These isotopes start with zero mass, accumulate to a maximum ('hump') near the middle of the life-cycle, and then depleted towards zero mass at the end of the life-cycle. The depletion of the trans-uranics occurs when their breeding source is depleted and decay and/or destruction dominates. The fission products deplete when their fission parents (or the fission parents of their decay parents, etc.) are depleted and decay and/or destruction dominates. ^{99}Tc (Figure 17) shows behavior that is typical of this class. The other fission products in this class are ^{147}Sm, ^{149}Sm, ^{151}Sm, ^{127}I, and ^{131}Xe. The trans-uranic isotopes are ^{237}Np, ^{236}Pu, ^{237}Pu, ^{238}Pu, ^{239}Pu, ^{240}Pu, ^{241}Pu, ^{242}Pu, ^{241}Am, ^{242}Am, ^{243}Am, ^{244}Am, ^{242}Cm, ^{243}Cm, ^{245}Cm. Additionally, the large thermal resonances in ^{152}Sm and ^{243}Pu cause them to be especially sensitive to perturbations in the ^{6}Li concentration, which competes as a strong thermal neutron absorber.

Several isotopes sit within a hybrid of the 'long-lived fission products' and 'hump isotopes' classes, peaking late in the life-cycle and quickly depleting towards mass at the very end. These isotopes possess a medium half-life (∼years) or a medium-low destruction cross-section (∼10–500 barns with significant resonances). Additionally, they may be extremely heavy (∼10 atomic masses higher than ^{238}U), which delays their peak mass. Their behavior occurs due to some combination of the physical effects of the two classes. ^{129}I (Figure 18) is a good example of the class which includes ^{128}Xe, ^{135}Cs, ^{150}Sm, ^{154}Sm, ^{244}Cm, ^{246}Cm, ^{247}Cm, and ^{248}Cm.

The class 'fresh fuel' contains the isotopes that are present at the beginning of the life-cycle, are bred or fissioned for the duration, and have essentially no decay or absorption sources. ^{238}U (Figure 26) is the primary example and ^{235}U (Figure 25) is a secondary example that depletes and then humps due to other sources (possibly a ^{238}Pu(n,α) reaction).

Another class 'breeding intermediates' contains isotopes that reside within the breeding chain and possess either an extremely short half-life (∼days or shorter) or a large destruction cross-section with prominent resonances. They exhibit 'stiff' behavior that tightly follows the mass their breeding parent. ^{239}U (Figure 27) is a great example among the others: ^{236}U, ^{237}U, ^{238}Np and ^{239}Np.

Similar to the previous class, 'short-lived fission products' are either extremely short-lived (∼days or hours) or have an extremely high destruction cross-section. This class differs from the previous in that they are produced through fission yield, not breeding and thus stiffly follow the power curve instead the mass of a breeding parent. ^{131}I (Figure 18) is a great example of the class which also includes ^{126}Sn errantly (more on this shortly), ^{135}I, ^{133}Xe, ^{135}Xe, and ^{153}Sm.

Bafflingly, ^{126}Sn (Figure 17) ended up in the 'short-lived fission products' class when in fact, it should be grouped among the 'long-lived fission products'. It has an extremely long half-life of ∼10,000 years and a low cross-section of ∼5–10 barns. Memos have been written that describe the issue in more detail [11] and then identify the error mechanism and solve it [12].

The last class 'tritium control isotopes' contains isotopes that are controlled for the purposes of creating $^{3}_{1}$H: ^{6}Li (Figure 16) and its isotope ^{7}Li (Figure 16).

Most isotope classes are sensitive to changes in temperature. The 'long-lived fission products' have similar fission yields from the various fission parents and thus vary only slightly during the breed-up and plateau portions of the life-cycle (but diverge during the tail portions).

The 'hump isotopes' peak higher at higher temperatures. This reflects accelerated production rates (fission for the fission products and capture for the trans-uranics). This is certainly true for ^{239}Pu, whose maximum mass increases by ∼40% for 300K→1500K (Figure 29). This is an important isotope since its mass is generally limited due to criticality and proliferation concerns as well as solubility concerns for the molten salt design. The isotopes that are hybrids of the 'long-lived fission products' and 'hump isotopes' classes respond to temperature at some intermediate degree.

The 'fresh fuel' isotopes behave as expected. ^{238}U is depleted at a faster rate at higher temperatures, corresponding to enhanced radiative capture. ^{235}U is depleted at a slower rate since thermal fluxes are starved from increased resonance capture.

The 'breeding intermediates' and 'short-lived fission products' are insensitive to temperature until the tail portions. For the former, this is because their sources and sinks are primarily resonance captures that respond to temperature in the same way. For the latter, this is because their sources and sinks are fission yield and decay, which are not sensitive to temperature.

5.3.4 Integral figures of merit

Within the Marcille data set, temperature variation brought only mild changes in resultant thermal power, burnup, and TBR. The slight differences in tritium breeding ratio (∼7% increase for 300K→1500K) enabled the higher temperature runs to produce more tritium at the same thermal power. Consequently, the higher temperature runs accumulated more tritium (∼40% higher @ ∼60kg for 1500K versus 300K) and thus operated at plateau thermal power for a larger portion of the life-cycle (60%→66% plateau time and 70%→76% energy produced within plateau for 300K→1500K). This resulted in a very slight time-advantage in achieving burnup (∼1.5 years for 80% FIMA, 1.75 years for 85% FIMA, and ∼2 years for 90% FIMA for 1500K versus 300K).

When comparing the results from using Song and Marcille nuclear data sets, one finds enormous discrepancies. At the very first transport calculation, before any depletion calculations were performed (and thus at identical isotopics), Song achieved a thermal power (700MW) that is ∼25%–60% larger. Simultaneously, Song achieved a TBR (∼1.18) that is ∼0%–17% higher. This allowed for an accelerated breed up to the plateau.

These extreme advantages that Song's data set bring enabled the maximum accumulation of ∼87 kg, or ∼40%–100% more tritium. Because of this, Song achieved balance of plant factors (fractional duration at plateau and fraction of energy generated at plateau) of ∼75% and ∼85% respectively, or approximately 12% higher than those using Marcille data. Additionally, Song had, on average, a ∼5%–7% faster rate of burnup and thus a burnup time-advantage for the duration of the life-cycle (∼1.2 years for 50%, ∼1.5 years for 60%, ∼1.7 years for 70%, ∼4.2 years for 80%, ∼7.8 years for 90%, and ∼9.7 years for 95%).

The 'tritium control isotopes' are sensitive to temperature. Since the $^{6}\mathrm{Li}(n,\alpha)T$ reaction is overwhelmingly thermal (Figure 5), the required density for a given TBR is sensitive to the thermal neutron flux (neutron thermalization is affected by moderator temperature (and density)).

5.4 Neutron Economy, Power Constraint, Sensitivity to Temperature

The neutron economy in a sub-critical LIFE engine is quite different from that within a thermal reactor. In Figure 7, one can see that virtually all of the neutrons in a thermal reactor are born through fission. The neutron economy and thermal power are therefore quite sensitive to reactivity. In a LIFE engine, however, fission accounts for only a portion of the neutrons–the rest being provided by (n,xn) reactions and an independent external fusion source. A moderate increase in fission neutrons represents a small increase in the overall neutron economy. Reactivity and thermal feedback's role in the overall neutron economy and thermal power is therefore smaller than in a thermal reactor.

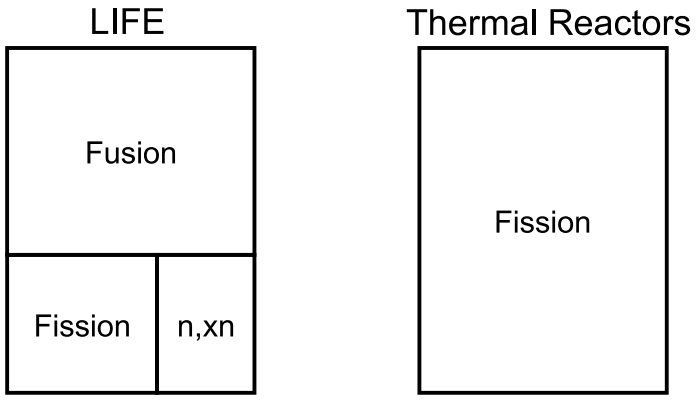

Note: Figure is not drawn to scale

Figure 7: Neutron economy (left) in a sub-critical LIFE engine and (right) a critical thermal reactor.

The thermal power in a LIFE engine during the plateau mode is constrained as constant. Really, this means that the sum of all the heating processes: fission, exothermic minus endothermic (non-fission) reactions, and neutron thermalization, are held constant as illustrated in Figure 8. While the sum is held constant, the relative amounts that each reaction contributes are free to change. Temperature changes can quietly change the neutron flux distribution–re-balancing reaction rates, and changing the isotopics while not affecting the thermal power.

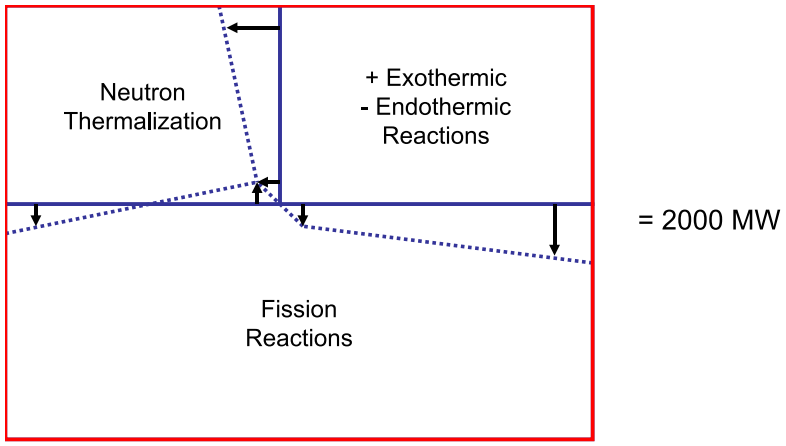

Note: Figure is not drawn to scale

Figure 8: Thermal heating contributions.

6 Conclusions

6.1 Marcille Nuclear Data

The nuclear data provided by Marcille agrees well with other data sets for criticality and achieves intuitively correct results with temperature variation. However, even after extensive scrubbing of the data files, many discrepancies exist in major aspects of the data: thermal power and tritium production. It should be noted that the LIFE engine control scheme may be re-balancing a single discrepancy to look like two discrepancies.

If a dataset is missing individual isotopes or reactions, it is inherently incomplete; no amount of verification and validation will fix the deficiencies and a brand new data set will be needed. Still, a thorough investigation of the discrepancies could be enlightening for the next time data is generated. Before any data set is considered for production use, it should be shown to contain all of the necessary reactions.

Differences in the included isotopes for each data set make alternating usage awkward.

6.2 LIFE's Sensitivity to Temperature

For the depleted uranium-fueled LIFE engine, all integral figures of merit except for TBR were only slightly sensitive to temperature. The differences in TBR resulted in altered tritium accumulation and exhaustion of tritium at different times, which changed the tail regions. Most notably of the results, almost all isotopics were sensitive to temperature due to the spectral effects upon cross-sections and neutron flux.

For this design, the reactor was deeply sub-critical, with negative Doppler coefficients for the entire life-cycle; criticality issues are benign. However, as the designs start encroaching upon criticality, reactivity will become more and more important, requiring accurate thermal modeling and feedback. Otherwise, it may be difficult to show that sub-criticality is maintained during the entire life-cycle in both nominal and accident conditions.

6.3 Figures of Merit to Investigate

Several aspects of LIFE were addressed with respect to their sensitivity to temperature: neutron flux, criticality, thermal power, tritium production, burnup, and isotopics. These figures of merit were not picked through an objective process that identified the mission critical state parameters of a LIFE design. Thus, there likely exist aspects that are a great deal more important; perhaps some time was wasted investigating irrelevant topics. Ideally, an objective top-down process that leverages the goals of a LIFE design would be used to identify only those physical processes that matter.

6.4 Recommended Fidelity

Assuming some degree of coupling is used in simulations, the current fidelity of TH calculation is likely sufficient for now. For the foreseeable future, the calculations will be significantly less expensive than the transport and depletion calculations. Running a TH simulation at too high a fidelity, too often, will not increase runtime significantly, regardless of whether the temperatures are fed back into the neutronics calculations.

Eventually, the intra-pebble and intra-kernel temperature distributions and pulsed behavior's distortions upon neutron flux will need to be addressed. When coupled simulations have different spatial grids, there will always be issues with homogenization that will have to be figured out: how does one obtain a homogenized temperature that preserves reaction rates?

6.5 Future Work

How temperature affects the isotopics of a molten salt reactor with online filtering of isotopes should be analyzed. A physically based, reaction rate-preserving homogenization scheme may be necessary. A top-down approach that identities the figures of merit that most affect the success of a LIFE design should guide the development of temperature modeling and feedback requirements. Multi-segmented shuffling schemes for power-flattening or thorium breeding will expose segments to different fluxes and different temperatures. How these interact should be addressed.

References

[1] DP Weber, T Sofu, SY Won, TJ Downar, JW Thomas, Z Zhong, JY Cho, KS Kim, TH Chun, HG Joo, and CH Kim. High-Fidelity Light Water Reactor Analysis With the Numerical Nuclear Reactor. Nuclear Science and Engineering, 155(3):395–408, 2007.

[2] JJ Duderstadt and LJ Hamilton. Nuclear Reactor Analysis. Number TK9202 .D77. John Wiley, New York, 1976.

[3] DE Cullen. Precision Temperature Dependent Results. Technical Report Memorandum, LLNL, Livermore (CA), 2007.

[4] RP Abbott. NIF-Wiki: LIFE Key Analyses (Mechanical), Blanket. `https://nif-wiki.llnl.gov/display/life/Blanket+(M)`, 2008.

[5] JE Seifried. Replacement of get_power With a Python Script; A Brief Timing Study. `https://nif-wiki.llnl.gov/display/life/SQA+Documents`, 2008.

[6] National Nuclear Data Center. Evaluated Nuclear Data File (ENDF). `http://www.nndc.bnl.gov/endf/`, 2006.

[7] LLNL Computational Nuclear Physics. Translated ENDF Formatted Data at LLNL. `http://nuclear.llnl.gov/CNP/translation/`, 2006.

[8] RE MacFarlane and DW Muir. The NJOY Nuclear Data Processing System Version 91. Technical Report LA-12740-M, LANL, 1994.

[9] JE Seifried. Comparison of LANL Cross-Section Libraries With Those of Peter Song. `https://nif-wiki.llnl.gov/display/life/SQA+Documents`, 2008.

[10] JE Seifried. Replacement of get_power With seifried.py in Life 0.4.*. `https://nif-wiki.llnl.gov/display/life/SQA+Documents`, 2008.

[11] JE Seifried. Description of suspicious mass results for Tin-126. `https://nif-wiki.llnl.gov/display/life/SQA+Documents`, 2009.

[12] JE Seifried. Description of Tin-126 mas error and a proposed solution. `https://nif-wiki.llnl.gov/display/life/SQA+Documents`, 2009.

A Energy-Dependent Results Graphs

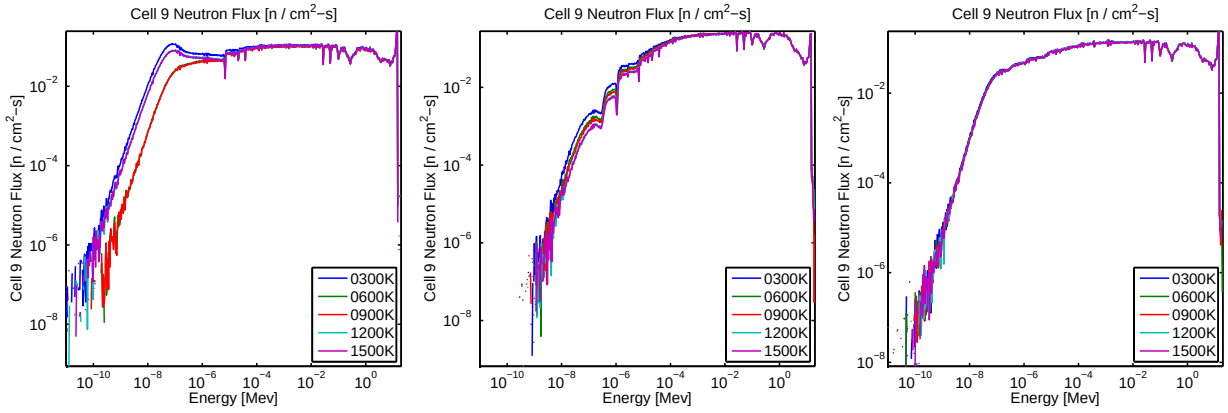

Figure 9: Energy-dependent neutron flux (left) at the beginning of life, (middle) maximum plutonium mass, and (right) 99% burnup.

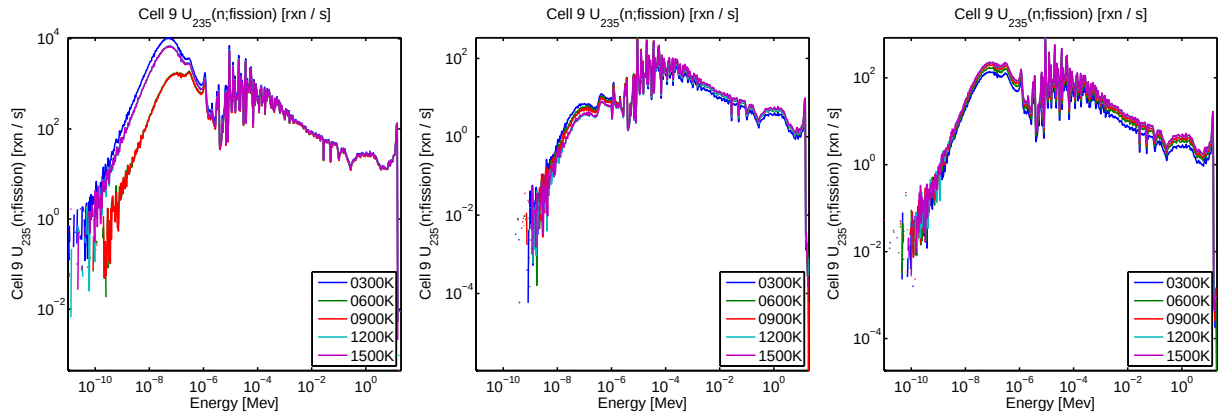

Figure 10: Energy-dependent Uranium-235 (n,fission) (left) at the beginning of life, (middle) maximum plutonium mass, and (right) 99% burnup.

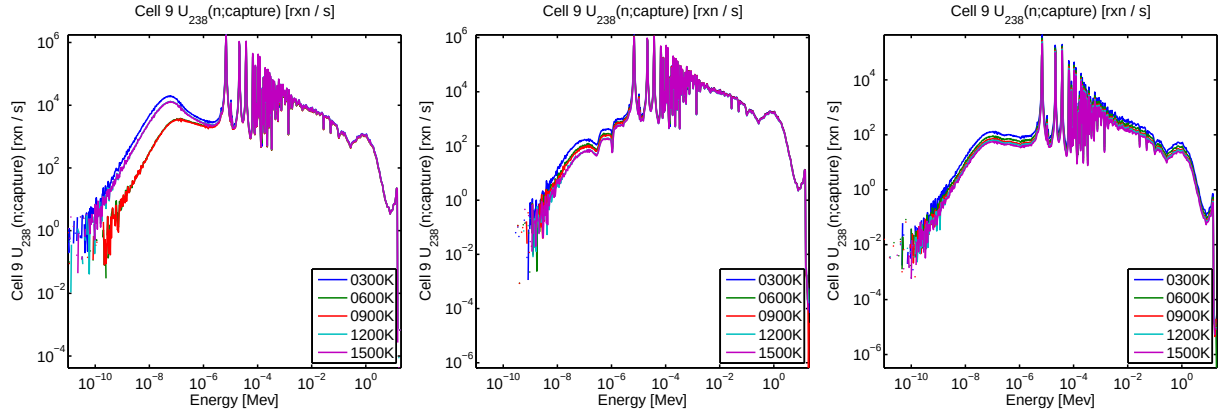

Figure 11: Energy-dependent Uranium-238 (n,capture) (left) at the beginning of life, (middle) maximum plutonium mass, and (right) 99% burnup.

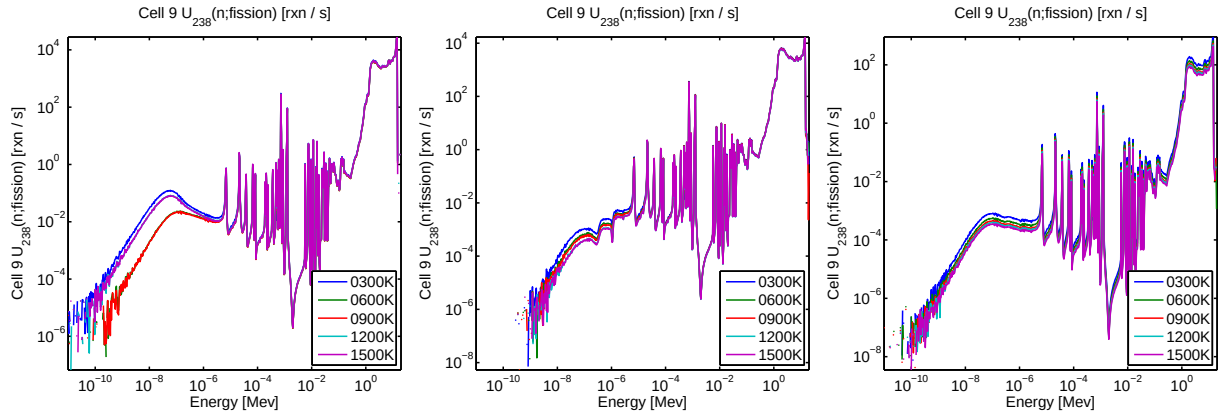

Figure 12: Energy-dependent Uranium-238 (n,fission) (left) at the beginning of life, (middle) maximum plutonium mass, and (right) 99% burnup.

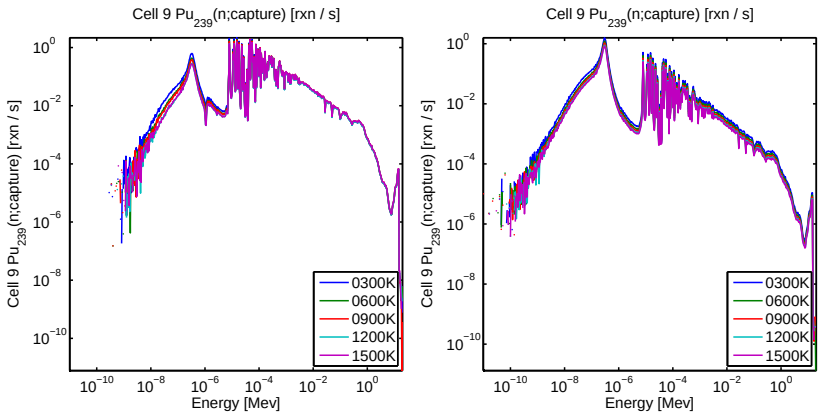

Figure 13: Energy-dependent Plutonium-239 (n,capture) (left) at the beginning of life, (middle) maximum plutonium mass, and (right) 99% burnup.

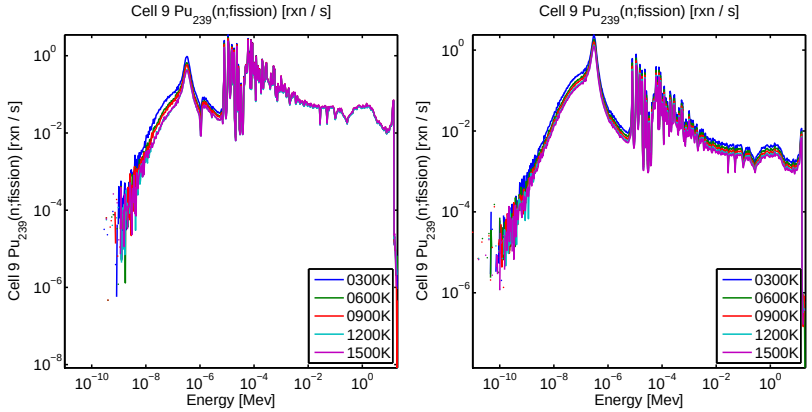

Figure 14: Energy-dependent Plutonium-239 (n,fission) (left) at the beginning of life, (middle) maximum plutonium mass, and (right) 99% burnup.

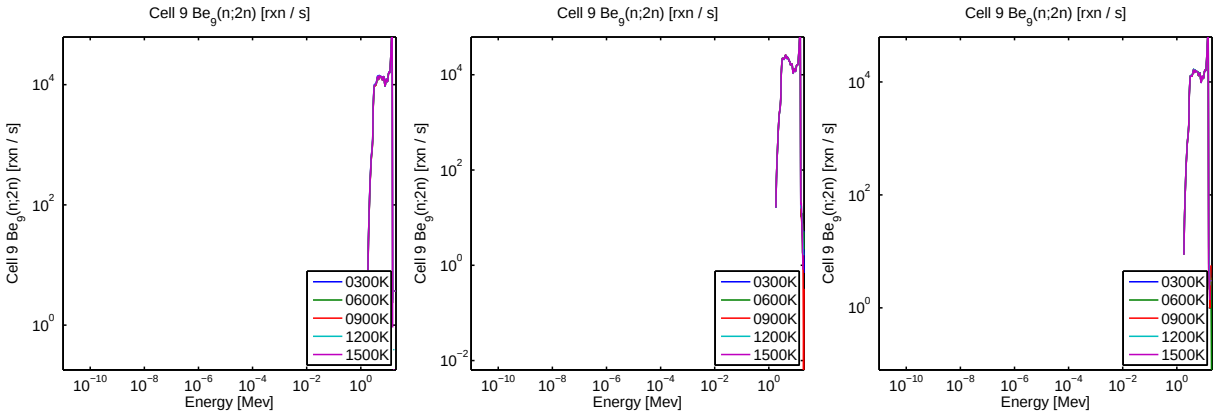

Figure 15: Energy-dependent Beryllium-9 (n,2n) (left) at the beginning of life, (middle) maximum plutonium mass, and (right) 99% burnup.

B Isotopic Results Graphs

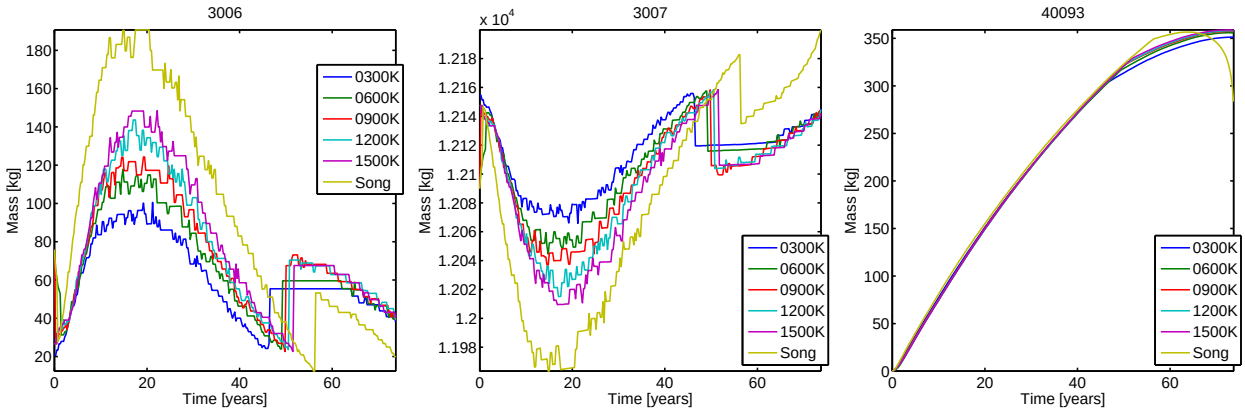

Figure 16: Mass versus time for (left) Lithium-6, (middle), Lithium-7, and (right) Zirconium-93 for various temperatures.

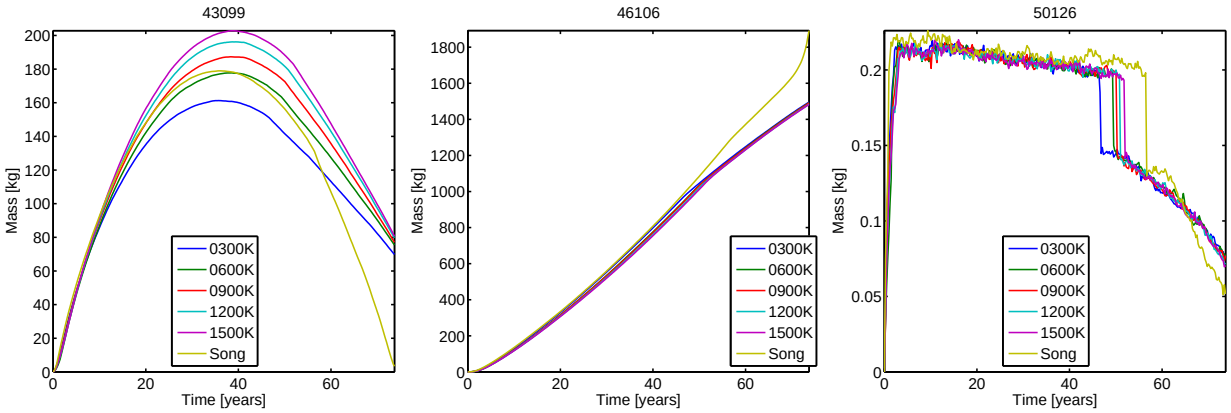

Figure 17: Mass versus time for (left) Technetium-99, (middle) Palladium-106, and (right) Tin-126 for various temperatures.

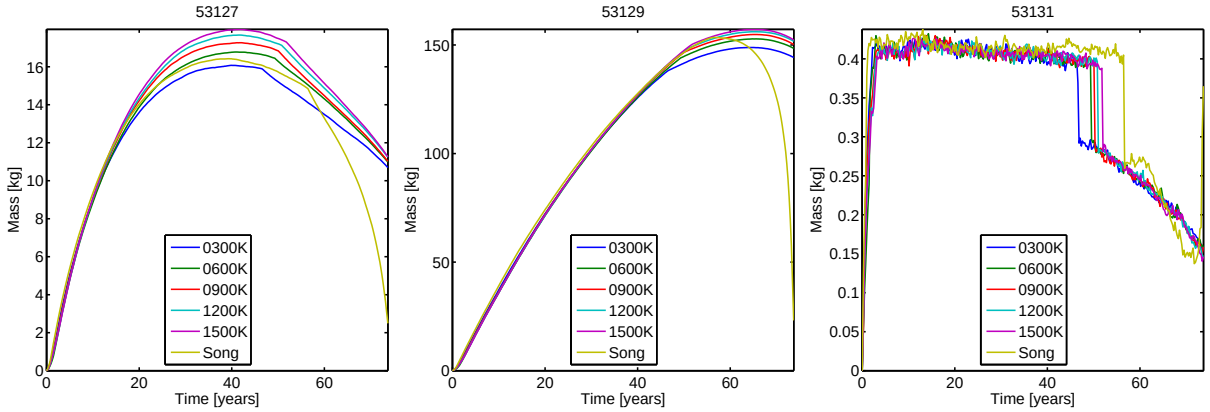

Figure 18: Mass versus time for (left) Iodine-127, (middle) Iodine-129, and (right) Iodine-131 for various temperatures.

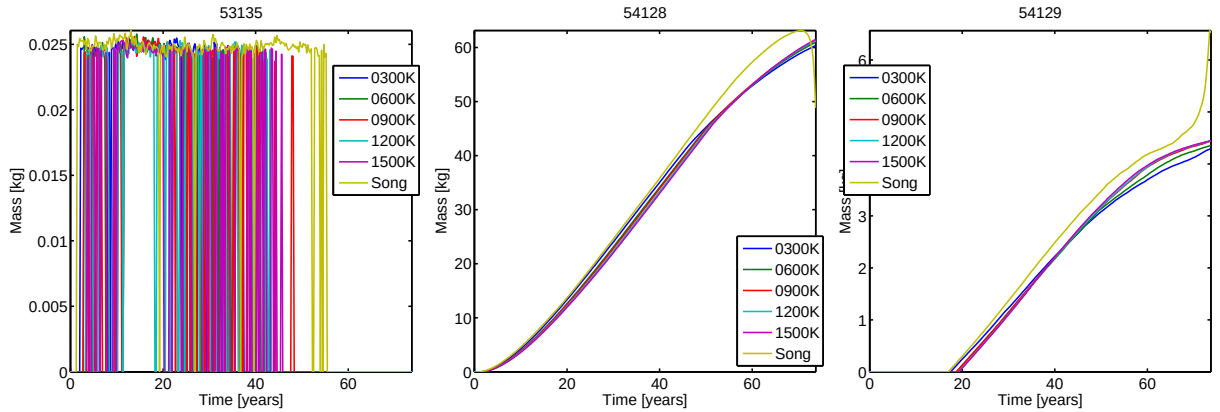

Figure 19: Mass versus time for (left) Iodine-135, (middle) Xenon-128, and (right) Xenon-129 for various temperatures.

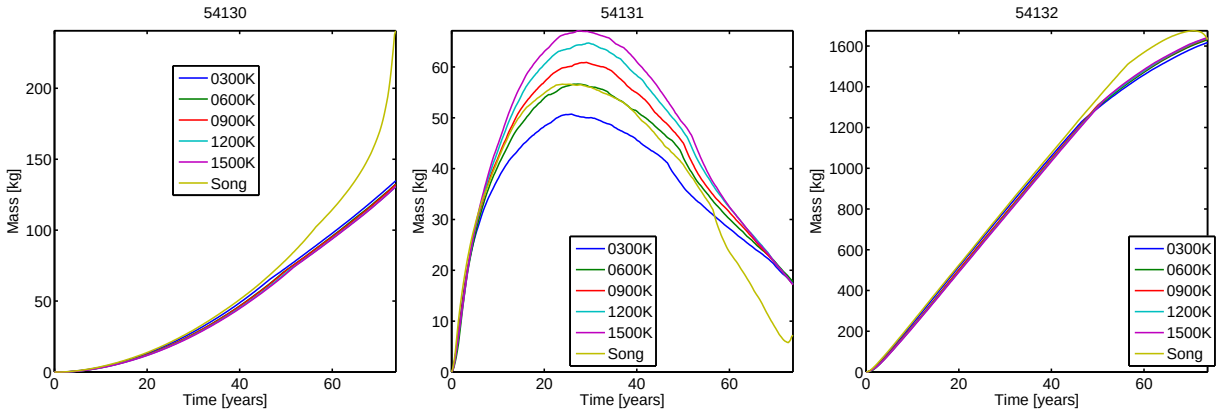

Figure 20: Mass versus time for (left) Xenon-130, (middle) Xenon-131, and (right) Xenon-132 for various temperatures.

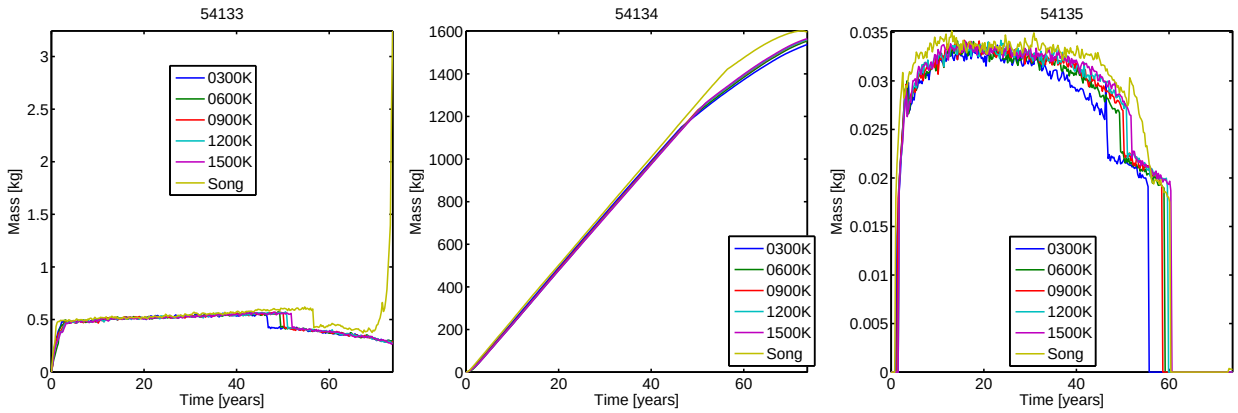

Figure 21: Mass versus time for (left) Xenon-133, (middle) Xenon-134, and (right) Xenon-135 for various temperatures.

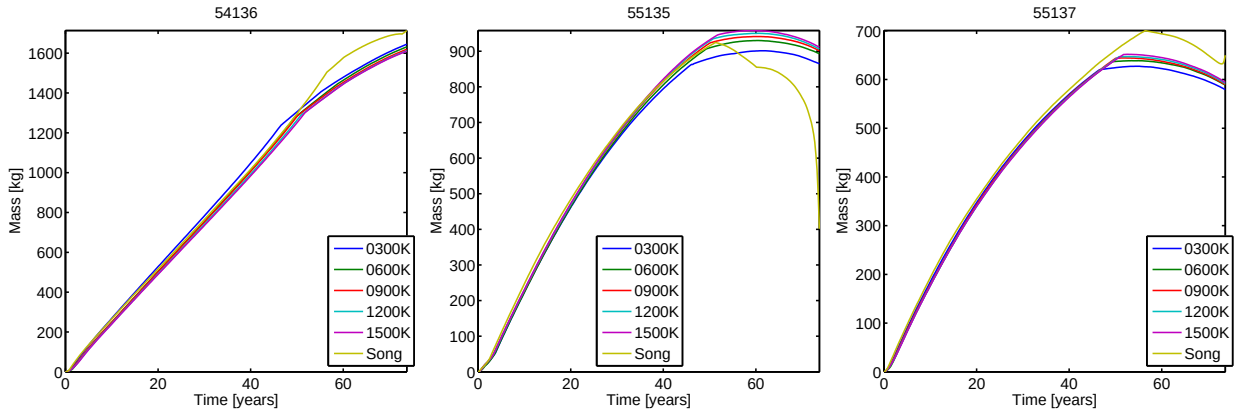

Figure 22: Mass versus time for (left) Xenon-136, (middle) Cesium-135, and (right) Cesium-137 for various temperatures.

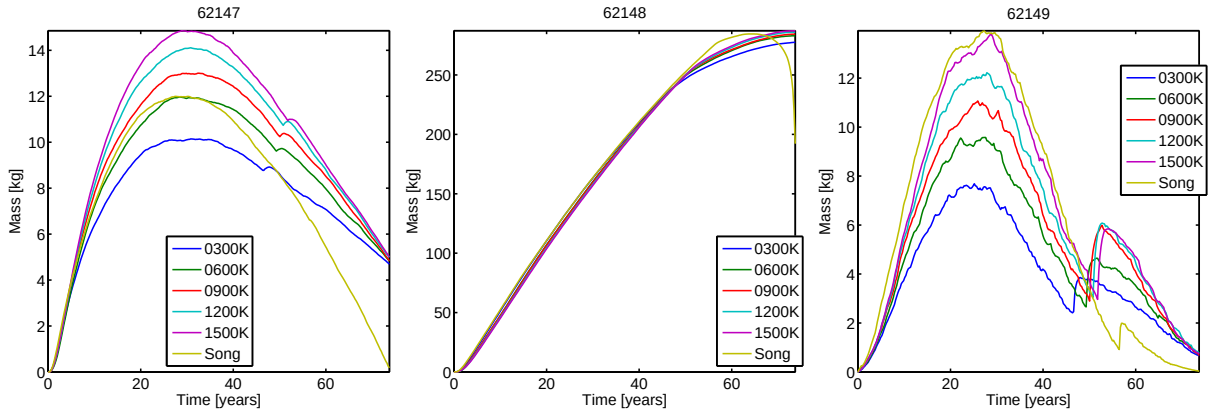

Figure 23: Mass versus time for (left) Samarium-147, (middle) Samarium-148, and (right) Samarium-149 for various temperatures.

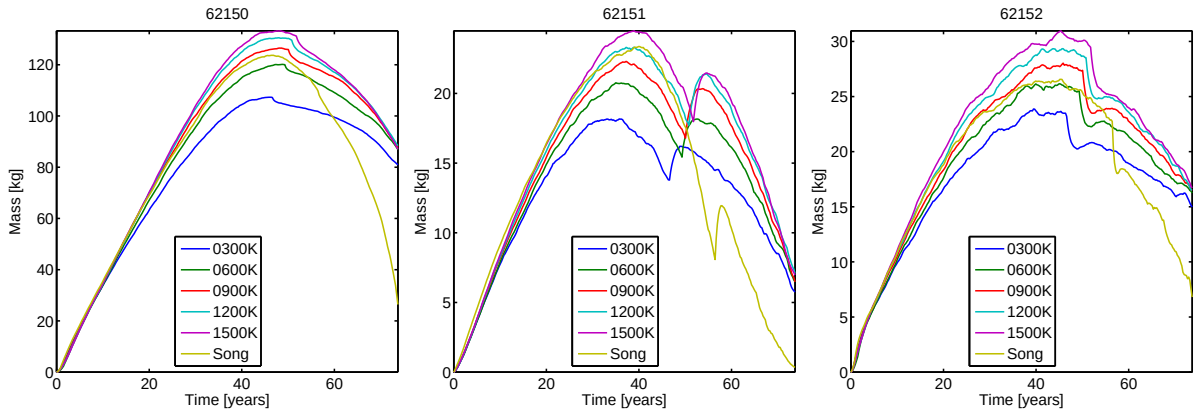

Figure 24: Mass versus time for (left) Samarium-150, (middle) Samarium-151, and (right) Samarium-152 for various temperatures.

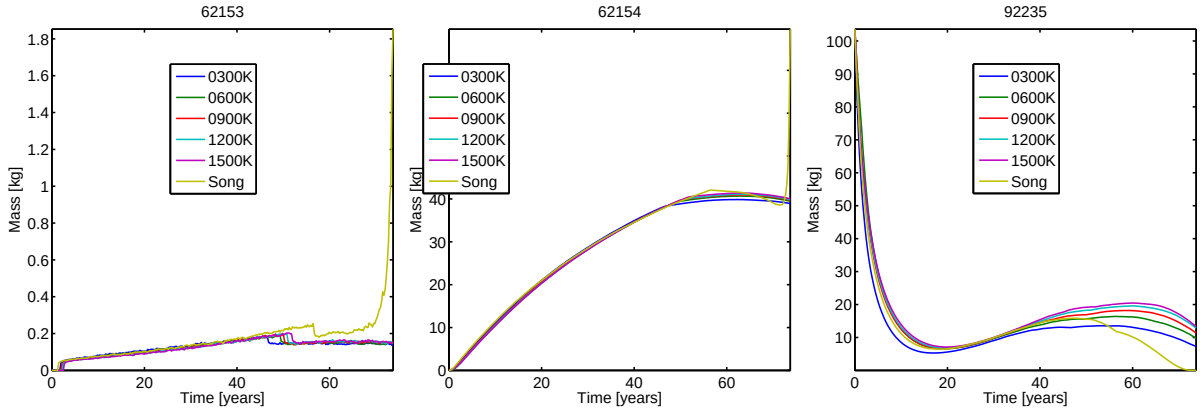

Figure 25: Mass versus time for (left) Samarium-153, (middle) Samarium-154, and (right) Uranium-235 for various temperatures.

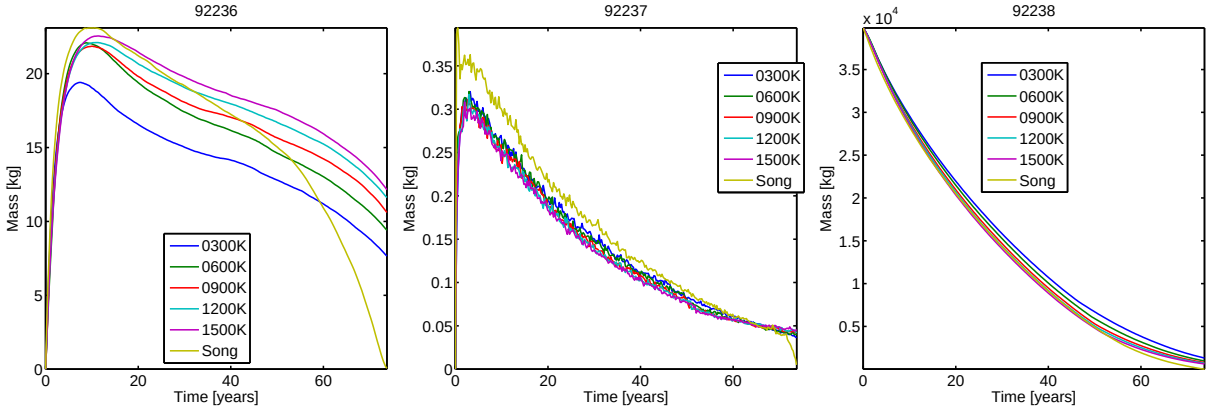

Figure 26: Mass versus time for (left) Uranium-236, (middle) Uranium-237, and (right) Uranium-238 for various temperatures.

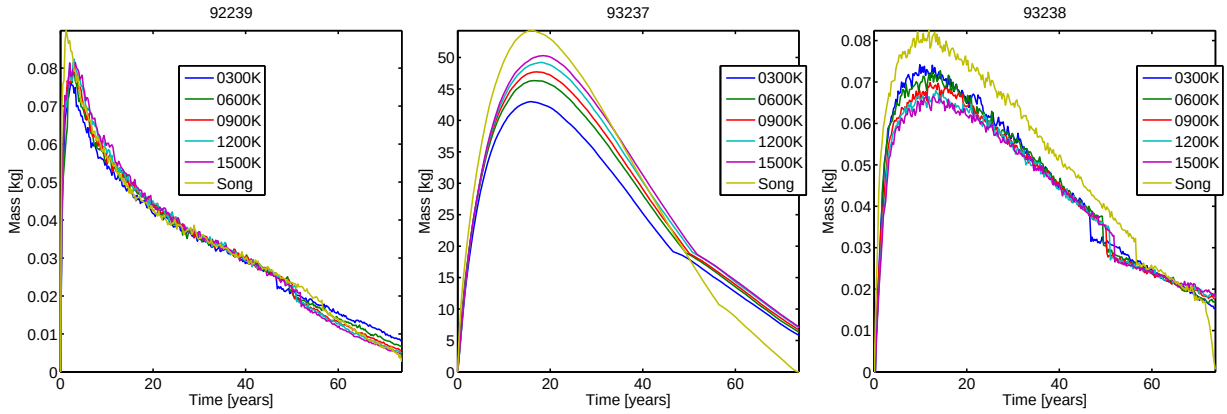

Figure 27: Mass versus time for (left) Neptunium-238, (middle) Uranium-239, and (right) Neptunium-237 for various temperatures.

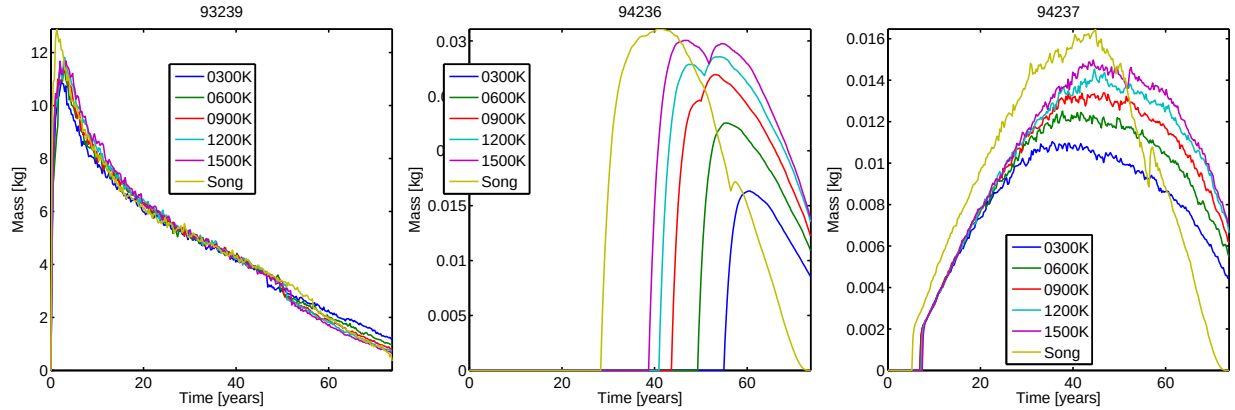

Figure 28: Mass versus time for (left) Neptunium-239, (middle) Plutonium-236, and (right) Plutonium-237 for various temperatures.

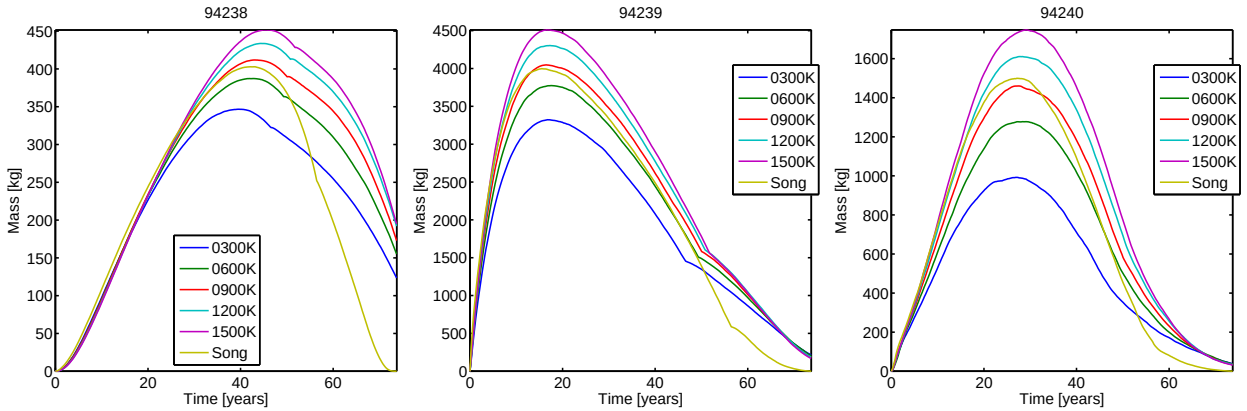

Figure 29: Mass versus time for (left) Plutonium-238, (middle) Plutonium-239, and (right) Plutonium-240 for various temperatures.

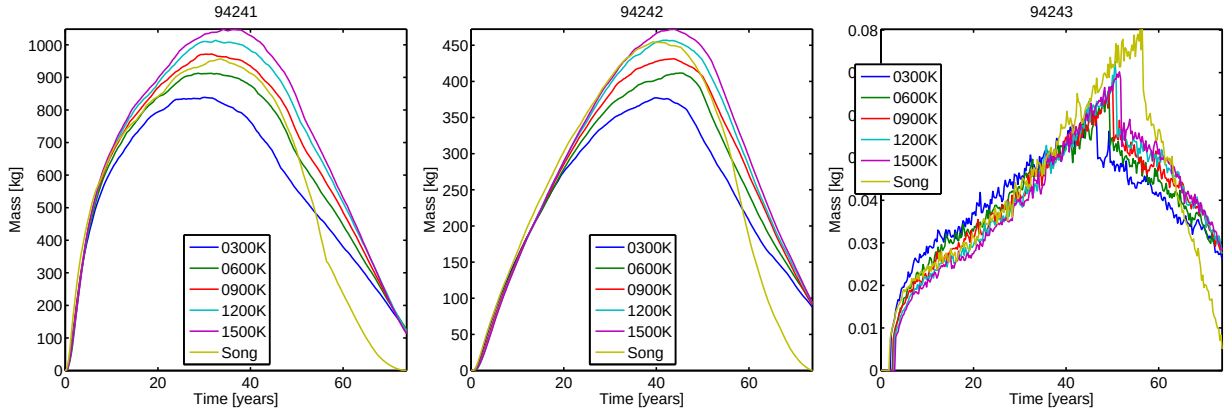

Figure 30: Mass versus time for (left) Plutonium-241, (middle) Plutonium-242, and (right) Plutonium-243 for various temperatures.

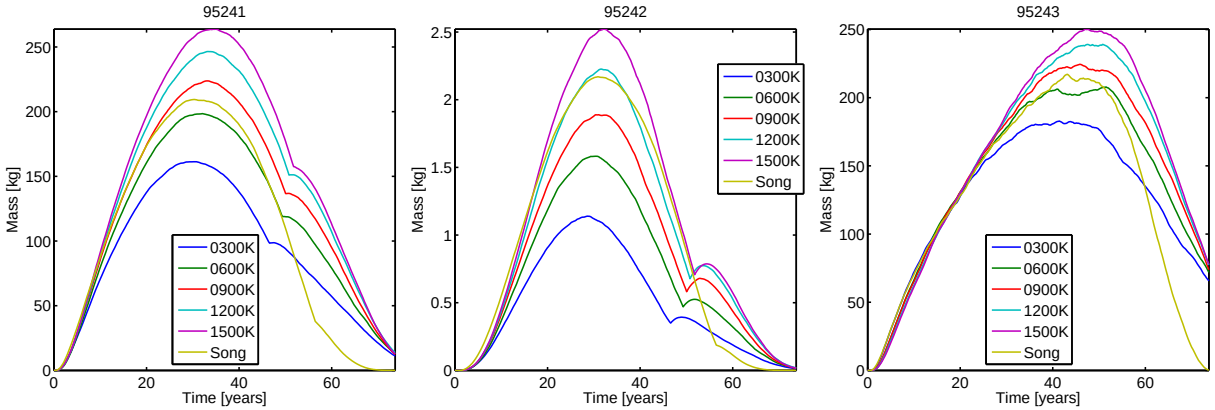

Figure 31: Mass versus time for (left) Americium-241, (middle) Americium-242, and (right) Americium-243 for various temperatures.

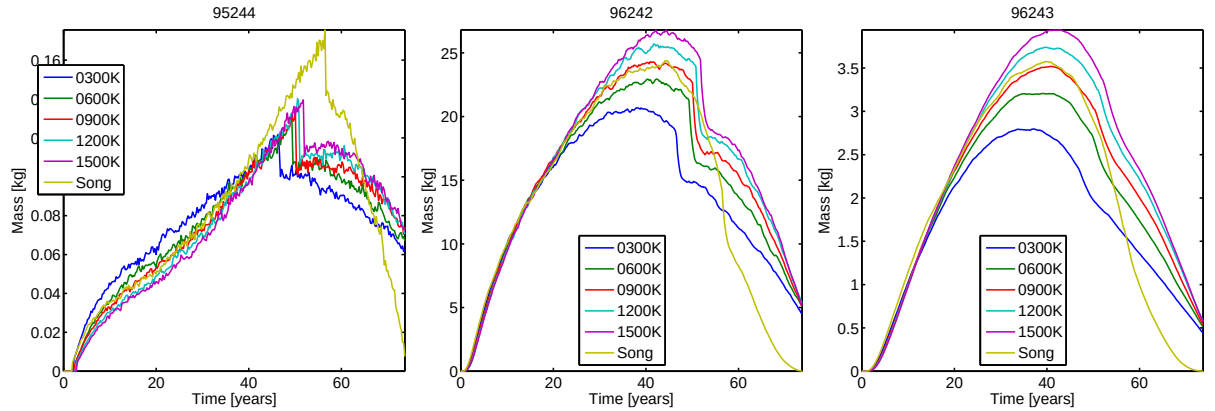

Figure 32: Mass versus time for (left) Americium-244, (middle) Curium-242, and (right) Curium-243 for various temperatures.

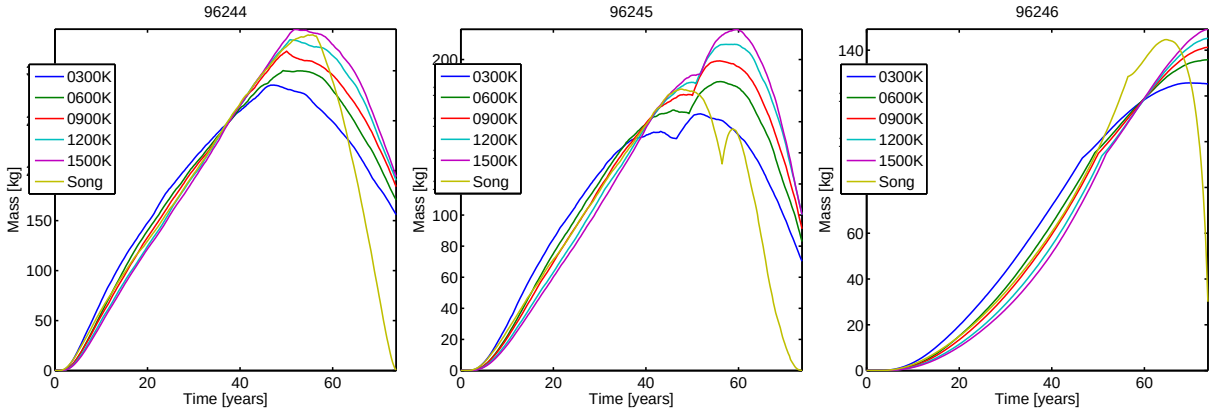

Figure 33: Mass versus time for (left) Curium-244, (middle) Curium-245, and (right) Curium-246 for various temperatures.

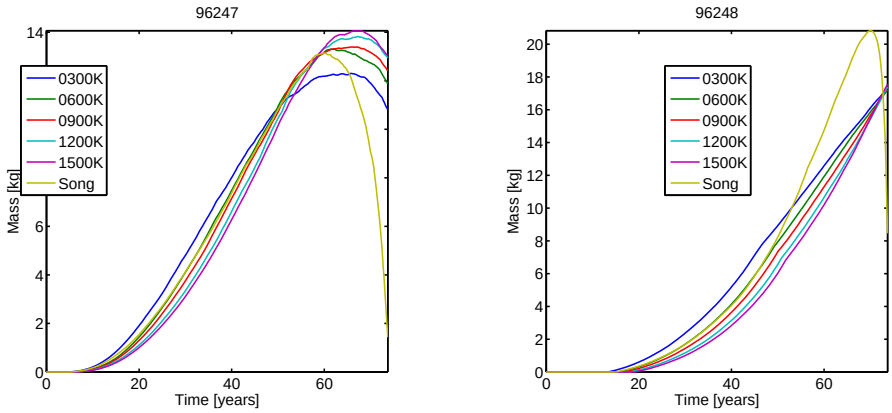

Figure 34: Mass versus time for (left) Curium-247 and (right) Curium-248 for various temperatures.

C Integral Results Graphs

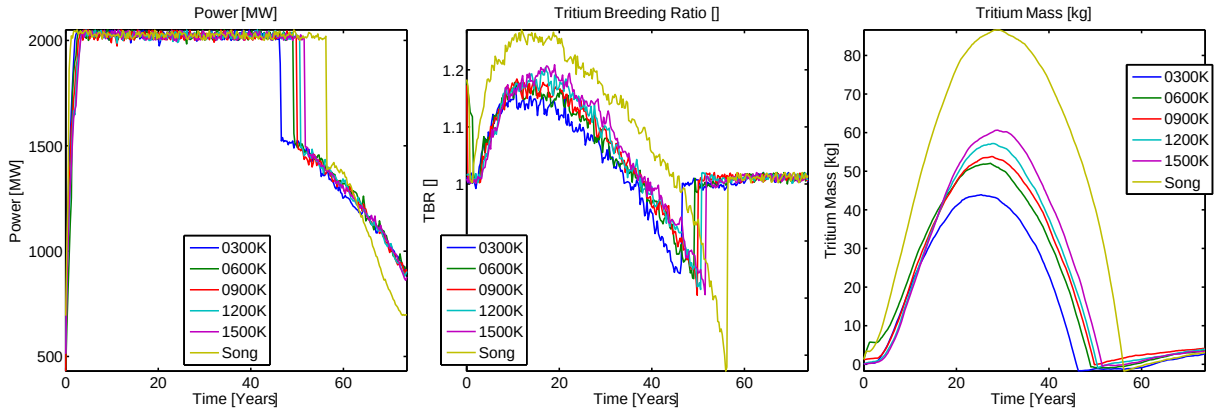

Figure 35: Integral figures of merit of (left) thermal power, (middle) tritium breeding ratio, and (right) Tritium Mass versus time for various temperatures.

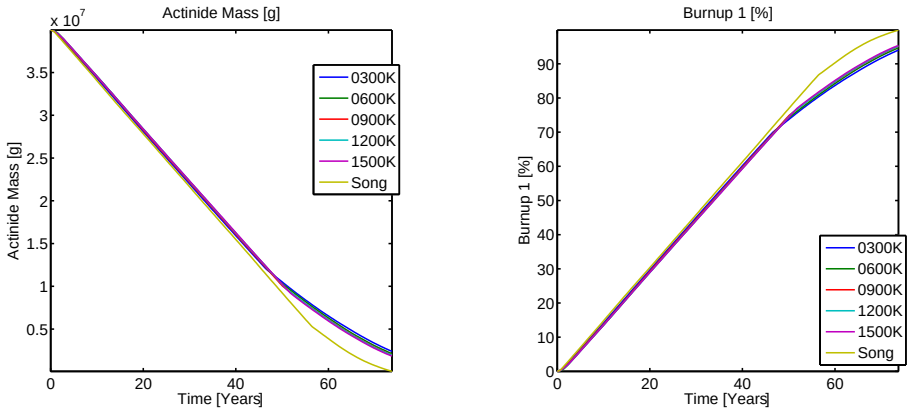

Figure 36: Integral figures of merit of (left) actinide mass and (right) burnup versus time for various temperatures.